



Published in final edited form as:

J Neurochem. 2010 February ; 112(3): 755–761. doi:10.1111/j.1471-4159.2009.06501.x.

Dysregulation of Intracellular Dopamine Stores Revealed in the R6/2 Mouse Striatum

Andrea N. Ortiz¹, Benjamin J. Kurth¹, Gregory L. Osterhaus¹, and Michael A. Johnson^{1,2}

¹Department of Chemistry and R. N. Adams Institute of Bioanalytical Chemistry, Lawrence, KS 66045 USA

²Neuroscience Program, Lawrence, KS 66045 USA

Abstract

Huntington's disease is a fatal, neurodegenerative movement disorder characterized by preferential and extensive striatal degeneration. Here, we used fast-scan cyclic voltammetry to study the mobilization and efflux of reserve pool dopamine in striatal brain slices from Huntington's disease model R6/2 mice. When applying stimulus trains of 120 pulses, evoked dopamine release in wild-type slices was greater than that in R6/2 slices at the higher frequencies (50 and 60 Hz). To quantify cytosolic and reserve pool dopamine levels, amphetamine-induced dopamine efflux was measured after pre-treatment with either tetrabenazine or alpha-methyl-tyrosine. Slices from 12-week old R6/2 mice released less dopamine than slices from wild-type mice, while no difference was noted in slices from 6-week old mice. The vesicular release of reserve pool dopamine, mobilized by treatment with cocaine, was shorter lived in R6/2 slices compared to wild-type slices even though peak dopamine release was the same. Moreover, the number of dopamine reserve pool vesicles in R6/2 mice was less than half of that in wild-type. Therefore, our data suggest that the same number of dopamine molecules are present in each reserve pool vesicle in WT and R6/2 mice and that these vesicles are readily mobilized in both genotypes; however, R6/2 mice have fewer dopamine reserve pool vesicles available for mobilization.

Keywords

Huntington's disease; dopamine; amphetamine; striatum; reserve pool; voltammetry

Introduction

Huntington's disease (HD) is an autosomal dominant neurodegenerative movement disorder caused by an expanded CAG repeat on the gene that encodes the huntingtin protein (htt). HD is characterized by mood disturbances, choreic movements, cognitive dysfunction, and degeneration of the striatum (Bates et al., 2002). Recent evidence indicates that impaired striatal dopamine (DA) release in HD rodent models contributes to the progressive motor

To whom correspondence should be addressed: Michael A. Johnson, The University of Kansas, Department of Chemistry, 1251 Wescoe Hall Drive, 2010 Malott Hall, Lawrence, KS 66047-7572, Telephone: (785) 864-4629, Fax: (785) 864-4629, johnsonm@ku.edu.

phenotype. This evidence includes: in vivo microdialysis studies in which DA levels in R6/1 and R6/2 mice were lower than that of wild type (WT) controls (Abercrombie and Russo, 2002; Petersén et al., 2002); locomotor measurements in which R6/2 mice had a blunted response to cocaine (COC) and methamphetamine (METH; Hickey et al., 2002; Johnson et al., 2006); and stimulated DA release measurements taken using fast-scan cyclic voltammetry (FSCV) in which release in R6/2 brain slices was impaired (Johnson et al., 2006; Johnson et al., 2007). Furthermore, amperometry data collected from adrenal chromaffin cells suggest that quantal release of catecholamines is diminished in R6/2 mice (Johnson et al., 2007). Nevertheless, specific mechanisms underlying presynaptic DA release impairments in striatal brain tissue have not yet been thoroughly investigated.

One potential mechanism of striatal dysfunction in R6/2 mice involves the mobilization of reserve pool DA. Vesicles containing DA are believed to be partitioned into three distinct pools. These pools include the readily releasable pool (RRP), which undergoes exocytosis upon mild stimulation, the recycling pool, which is mobilized to replace RRP vesicles, and the reserve pool, which is thought to be mobilized during periods of prolonged synaptic activity (Neves and Lagnado, 1999; Zucker and Regehr, 2002; Rizzoli and Betz, 2005). The reserve pool is the largest vesicle pool, consisting of ~80–90% of the total vesicles in presynaptic terminals (Neves and Lagnado, 1999; Rizzoli and Betz, 2005). It has been shown previously that a synapsin-dependent DA reserve pool can be mobilized by treatment with COC (Venton et al., 2006). Thus, not only does this study suggest a possible mechanism for the attenuated psychostimulatory effect of COC in R6/2 mice, but it also identifies a mechanism by which DA reserve pools can be pharmacologically manipulated.

In this work, we investigated the neurochemical mechanisms that underlie striatal DA release impairments, which could potentially amplify phenotypical behavioral impairments observed in R6/2 mice (Carter *et al.* 1999). We hypothesized that reserve pool DA is depleted in R6/2 mice. To investigate this possibility, FSCV was used to measure amphetamine (AMPH) induced efflux and COC-induced vesicle mobilization of reserve pool DA in acute striatal slices from R6/2 and WT control mice. Our results suggest not only that the amount of striatal reserve dopamine is diminished in R6/2 mice, but also that this decrease is associated with a decline in the number of DA reserve pool vesicles available for mobilization.

Materials and Methods

Drugs

COC, αMPT, and AMPH were purchased from Sigma-Aldrich (St. Louis, MO). Tetrabenazine (TBZ) was a generous gift from Prof. Eric Floors, Department of Molecular Biosciences, University of Kansas.

Animals

R6/2 [B6CBA-Tg(HDexon1)62Gpb] and wild-type mice were purchased from Jackson Laboratories (Bar Harbor, Maine) and were housed at the University of Kansas animal care unit prior to use. Food and water were provided ad libitum and a 12-hour light-dark cycle

was used. All animal procedures were approved by the Institutional Animal Care and Use Committee.

Brain Slice Preparation

Brain slices were prepared as previously described (Johnson et al., 2006). Briefly, mice were anesthetized by isoflurane inhalation and then decapitated. The brain was immediately removed and placed in ice cold artificial cerebrospinal fluid (aCSF). The aCSF consisted of 126 mM NaCl, 2.5 mM KCl, 1.2 mM NaH₂PO₄, 2.4 mM CaCl₂, 1.2 mM MgCl₂, 25 mM NaHCO₃, 20 mM HEPES, and 11 mM D-Glucose. The pH was adjusted to 7.4. During the brain slice harvesting procedure and during experimentation, the aCSF was continuously saturated with 95% O₂/5% CO₂. The cerebellum was sliced off with a razor blade and then the brain was mounted on an aluminum block. Coronal slices, 300 μm thick, were made using a vibratome slicer (Leica, Wetzlar, Germany). Brain slices containing striata were stored in ice cold aCSF. A single slice was placed in the superfusion chamber, through which aCSF, maintained at 34° C, flowed at a continuous rate of 2 mL/min. Each brain slice was equilibrated in the superfusion chamber for 60 minutes prior to obtaining measurements. To apply αMPT, TBZ, AMPH, and COC, aCSF containing these drugs was maintained in a separate reservoir and introduced through a three-way valve.

DA release in brain slices

Carbon-fiber microelectrodes were fabricated as previously described (Kraft et al., 2009), with minor changes. Briefly, a single 7 μm diameter carbon-fiber (Goodfellow Cambridge Ltd, Huntingdon, U.K.) was aspirated through a glass capillary tube (1.2 mm outer diameter, 0.68 mm inner diameter, 4 inches long, A-M Systems, Inc. Carlsborg, WA, USA), which was pulled using a heated coil puller (Narishige International USA, Inc., East Meadow, NY). Electrodes were trimmed to 25 μm from the glass seal, further insulated with epoxy resin (EPON resin 815C, EPIKURE 3234 curing agent, Miller-Stephenson, Danbury, CT, USA), and then cured at 100°C for 1 h. Prior to experimentation, electrodes were backfilled with 0.5 M potassium acetate in order to provide an electrical connection between the carbon fiber and an inserted silver wire. No further treatment of the electroactive surface was performed.

A triangular waveform, starting at -0.4 V, increasing to +1.0 V, and then scanning back to -0.4 V, was applied at the carbon-fiber working electrode. A scan rate of 300 V/s was used with an update rate of 60 Hz for single pulse stimulations and 10 Hz for 120-pulse stimulations. A headstage amplifier (UNC Chemistry Department Electronics Design Facility, Chapel Hill, NC) was interfaced with a computer via a breakout box and custom software provided by R.M. Wightman and M.L.A.V. Heien, University of North Carolina, Chapel Hill. A chlorided silver wire was used as an Ag/AgCl reference electrode. The carbon fiber microelectrode was inserted 100 μm into the dorsolateral caudate-putamen region of the striatum between the prongs of a bipolar stimulation electrode (Plastics One, Roanoke, VA), which was separated by a distance of 200 μm. The current was then measured at the peak oxidation potential for dopamine (about +0.6V versus Ag/AgCl reference electrode). For the 120-pulse stimulations, DA release was measured using stimulation frequencies of 20, 30, 40, 50, and 60 Hz at four locations in the dorsolateral

striatum. At each location the DA release was measured going from the lowest frequency (20 Hz) to the highest frequency (60 Hz) with a 5 minute recovery time between each measurement. Working electrodes were calibrated with dopamine standards of known concentration in a flow cell before and after each use. The average of the pre and post calibration measurements was used as the calibration factor.

For DA efflux studies, single stimulus pulses were applied every five minutes until peak dopamine release was consistent over three consecutive measurements. Once the DA release was consistent, either 50 μM αMPT or 10 μM TBZ was added to the aCSF. The brain slice was stimulated every 5 minutes until the DA release peak disappeared. Next, 20 μM AMPH was introduced into the aCSF perfusion solution in addition to the αMPT or TBZ that was already present. AMPH-induced efflux was then measured without the use of electrical stimulation over the course of 25 minutes with an update rate of 5 Hz. This update rate was used in order to limit the amount of memory required for storage of the file. These data were also background-subtracted and collected at the same scan rate and potential limits as the stimulated release data. For studies using COC, the previous procedure for αMPT was followed except that once the DA release peak disappeared, 20 μM COC was added to the αMPT solution and we continued to apply the single stimulus pulses every 5 minutes. Stimulus pulses were applied for up to 120 minutes in this case in order to capture the increase and eventual decrease in stimulated release.

Data Analysis

For statistical comparisons, GraphPad Prism (version 4.03) software was used. Data are expressed as a mean \pm SEM. A one-way analysis of variance with repeated measures statistical test was used to assess within-genotype influences of stimulation frequency on DA release (Fig. 1). Other comparisons were assessed by unpaired Student's t-test with $p < 0.05$ being considered significant.

Results

Striatal DA Release

It has previously been shown using striatal brain slice preparations that upon single pulse electrical stimulation, 12-week old R6/2 mice release significantly less DA than their age-matched WT controls (Johnson et al., 2006). To investigate the impact of the HD mutation on DA reserve pool mobilization, slices from 12-week old R6/2 and WT mice were subjected to 120-pulse stimulations at 20, 30, 40, 50, and 60 Hz, and FSCV at carbon fiber microelectrodes was used to measure DA release (Fig. 1A). Cyclic voltammograms obtained at the highest point of stimulated release ($[\text{DA}]_{\text{stim}}$) confirm that the analyte detected is dopamine. Although the DA release in WT slices appears to increase as frequency is increased, there was no statistically significant difference between stimulation frequencies (Fig. 1B; ANOVA). However, at 50 and 60 Hz stimulation frequencies, $[\text{DA}]_{\text{stim}}$ was significantly less in R6/2 slices than in WT slices ($p < 0.05$ at both frequencies). The average values for $[\text{DA}]_{\text{stim}}$ at 50 Hz were $1.20 \pm 0.33 \mu\text{M}$ (R6/2; $n = 5$ mice) and $2.71 \pm 0.47 \mu\text{M}$ (WT; $n = 6$ mice). At 60 Hz, the values were $1.31 \pm 0.32 \mu\text{M}$ (R6/2; $n = 5$ mice) and $3.34 \pm 0.76 \mu\text{M}$ (WT; $n = 6$ mice).

Intracellular DA Levels

The aforementioned stimulated release results shown in Fig. 1 prompted us to determine the relative amounts of DA found in pharmacologically distinct pools. Amphetamine-induced DA efflux measurements in brain slices of 6-week and 12-week R6/2 and WT mice were compared. Each slice was continuously treated with 10 μM TBZ, which blocks the loading of DA into vesicles by inhibiting VMAT (Kung *et al.* 1994). RRP dopamine was then depleted by applying single-pulse stimulations every five minutes until the stimulated release peak disappeared. At this point, the only dopamine remaining in the terminals was reserve pool and free cytosolic DA. Slices were then exposed to 20 μM AMPH, a competitive dopamine transporter (DAT) inhibitor that causes DA efflux from vesicles inside presynaptic terminals. AMPH enters presynaptic terminals either by lipophilic diffusion through membranes or by passage through DAT protein molecules. AMPH that enters through DAT causes allosteric translocation of the transporters and thereby induces reverse transport of DA from the cytoplasm (Liang & Rutledge 1982, Fischer & Cho 1979). AMPH also displaces vesicular DA into the cytoplasm where it can then be released by reverse transport (Chiuueh & Moore 1975, Jones *et al.* 1998). Therefore, we used AMPH as a pharmacological tool for emptying DA from presynaptic terminals into the extracellular space. The efflux of DA was measured over the course of 25 minutes. The amplitude of the peak ($[\text{DA}]_{\text{AMPH}}$) was used to determine the amount of DA released (Fig. 2A). In six-week old R6/2 and WT mice there was not a significant difference in the amount of AMPH induced efflux of DA (R6/2, $11.49 \pm 2.36 \mu\text{M}$, $n = 6$ mice; WT, $12.41 \pm 2.26 \mu\text{M}$, $n = 7$ mice). However, by 12 weeks of age, the R6/2 mice showed a significant decrease in AMPH-induced DA efflux after TBZ treatment (Fig. 2B; $p = 0.023$; R6/2, $5.41 \pm 1.10 \mu\text{M}$, $n = 7$ mice; WT, $10.44 \pm 1.65 \mu\text{M}$, $n = 8$ mice).

To measure reserve pool DA more selectively, a separate set of experiments were conducted in which slices were treated with αMPT rather than TBZ. αMPT inhibits tyrosine hydroxylase, the rate limiting enzyme in DA synthesis. A stimulus pulse was applied every 5 minutes until the DA peak disappeared, and then AMPH was added to the aCSF perfusion solution, in addition to the 50 μM αMPT , at a final concentration of 20 μM . The peak amplitude of the AMPH-induced efflux, $[\text{DA}]_{\text{AMPH}}$, was measured to quantify the amount of DA stored in reserve pool vesicles (Fig. 3). At 6 weeks of age, there was not a significant difference between R6/2 and WT mice (R6/2, $8.17 \pm 1.96 \mu\text{M}$, $n = 5$ mice; WT, $5.39 \pm 0.88 \mu\text{M}$, $n = 3$ mice). Conversely, $[\text{DA}]_{\text{AMPH}}$ was diminished in slices from 12-week old R6/2 mice compared to age-matched WT controls ($p < 0.05$; R6/2, $4.02 \pm 0.74 \mu\text{M}$, $n = 5$ mice; WT, $7.75 \pm 1.48 \mu\text{M}$, $n = 4$ mice).

Mobilization of Reserve Pool DA

To determine if reserve pool DA is mobilized differently in older R6/2 mice compared to age-matched WT control mice, αMPT and then COC, which has been shown to mobilize DA reserve pools (Venton *et al.*, 2006), were added sequentially to the perfusion solution while measuring stimulated DA release. First, DA release, evoked by the application of single electrical stimulus pulses, was measured using FSCV in striatal brain slices from 12-week old R6/2 and WT mice. The pulses were applied prior to and throughout the pharmacological treatment of each slice. Next, slices were treated with 50 μM αMPT .

Finally, once the stimulated DA release peak disappeared, slices were treated with 20 μM COC in addition to the αMPT . The WT slices released DA for a longer period of time (90 min) after the addition of COC in comparison to R6/2 slices (30 min; Fig. 4A). The maximum COC-induced DA release was not significantly different between the R6/2 and WT mice (Fig. 4B). Area under the curve calculations suggest that the R6/2 slices released DA from fewer vesicles (41.6% of WT).

Discussion

In this study, differences in DA reserve pool storage and mobilization in striatal brain slices from R6/2 and WT mice were examined. In R6/2 slices, electrically-induced release of dopamine was non-responsive to increasing stimulation frequencies. However, release from WT slices was significantly greater than that in R6/2 slices at the higher stimulation frequencies. Moreover, AMPH-induced DA efflux was diminished in slices from R6/2 mice at 12 weeks of age, but not at 6 weeks of age, indicative of an age-dependent deficit of reserve pool DA in R6/2 mice. Our data also suggest that fewer DA reserve pool vesicles were mobilized in slices from 12-week old R6/2 mice compared to slices from age-matched WT control mice; thus, fewer reserve pool vesicles are present in the R6/2 striatum.

Previous studies using R6/2 mice have shown that DA release, evoked using a single pulse stimulation, is impaired in brain slices from 12-week old R6/2 mice (Johnson et al., 2006). This single pulse application causes DA to be released from the RRP which makes up only 1 to 2% of vesicles in presynaptic terminals (Rizzoli and Betz, 2005). Similarly, electrically evoked release of DA using the 120-pulse stimulation regimen was diminished in R6/2 slices at the higher stimulation frequencies (50 and 60Hz) but not at the lower frequencies (20, 30, and 40 HZ). Even though peak dopamine levels were observed after the application of about 18 pulses at 60 Hz and 15 pulses at 50 Hz, a full 120 pulse regimen was applied in an attempt to reveal genotype-related differences. A difference in [DA] between R6/2 and WT at the end of this pulse regimen could potentially suggest a difference in the ability to sustain dopamine release during periods of excessive stimulation. However, there was not a significant difference between the R6/2 and WT mice. Given that the reserve pool makes up 80 to 90% of vesicular DA stores (Neves and Lagnado, 1999; Rizzoli and Betz, 2005), it seems likely that, if these stores were mobilized, they would overwhelm and mask the release of RRP DA. Indeed, the average magnitude of DA release, evoked by the application of a 120-pulse train, was on the order of 3 to 4 μM from WT slices compared to about 1.5 μM evoked by application of a single stimulus pulse (Johnson et al., 2006). Thus, it is possible that the difference in DA release between the R6/2 and WT mice at high stimulation frequencies is driven by the mobilization of stored pool vesicles. According to the standard three pool model, the vesicles in the RRP are released first upon mild stimulation in which the axon terminal is depolarized by an action potential (Wu and Borst, 1999). As the RRP becomes depleted, the recycle pool vesicles mobilize (Harata et al., 2001; de Lange et al., 2003; Kuromi and Kidokoro, 2003; Richards et al., 2003). Upon frequent or more intense stimulation, the reserve pool vesicles mobilize (Richards et al., 2000; Richards et al., 2003; Heien and Wightman, 2006). It has been shown that, in anesthetized rats, reserve pool DA can be mobilized by stimulating the medial forebrain

bundle at 5-second intervals using a stimulating frequency of 30 Hz (Yavich and MacDonald, 2000).

Phasic DA signaling is important for the expression of behavior (Heien and Wightman, 2006). However, it is also important to note that input from cortical glutamate afferents may exert control over behavior by driving striatal medium spiny neuron firing (Lape and Dani, 2004) and influencing DA release (Kulagina et al., 2001; Avshalumov et al., 2003). Tonic DA levels have been proposed to restrain the excitatory effects of glutamate input by acting primarily on dopaminergic D1 receptors (Kiyatkin and Rebec, 1999). The lower stimulation frequencies (20 or 30 Hz) are associated more with tonic DA levels in the striatum (Hyland et al., 2002; Heien and Wightman, 2006); therefore, because DA release was not significantly different between R6/2 and WT at these frequencies, it appears unlikely that differences in tonic dopamine levels play a major role in the propagation of abnormal behaviors in these mice. Conversely, phasic bursts of DA may be associated with upper stimulation frequencies (50 and 60 Hz); therefore, it is possible that 12-week old R6/2 mice lack the ability to provide the needed phasic dopaminergic input required for normal motor control, thereby contributing to the abnormal behavioral phenotype.

The DA reserve pools were examined using various pharmacological agents. Treating the brain slices with TBZ coupled with electrical stimulation will deplete the releasable vesicles. Upon the addition of AMPH intracellular and vesicular DA will exit the terminals by reverse transport through the DAT into the extracellular space (Sulzer et al., 1995; Floor and Meng, 1996; Jones et al., 1998; Schwartz et al., 2005; Watanabe et al., 2005). The diminished DA efflux in 12-week old R6/2 mice indicates that DA, not released by stimulation with a single electrical pulse, becomes progressively depleted between 6 and 12 weeks of age. This DA is made up of reserve pool DA and free cytosolic DA. Similar results were obtained when reserve pool DA was selectively isolated by treatment of slices with α MPT, which, when combined with electrical stimulation, depletes releasable DA stores and free cytosolic DA. R6/2 mice typically develop the overt motor phenotype at 9 to 11 weeks of age; thus, the timescale of reserve pool depletion is consistent with the occurrence of motor symptoms.

More commonly known as a dopamine uptake inhibitor, COC has a similar affinity for DAT in R6/2 mice as compared to WT mice (Johnson et al, 2006). Thus, the differences in release measured after treating R6/2 and WT slices with COC following pre-treatment with α MPT most likely arise from differences in the stimulated release of the mobilized DA reserve pool, not differences in uptake. Because the peak DA levels evoked by single pulse electrical stimulation are the same in R6/2 and WT control slices under these conditions, it is likely that R6/2 mice can mobilize reserve pool vesicles normally, and that the vesicles contain the same number of DA molecules. These results also imply that there are similar densities of DA-releasing presynaptic terminals in the R6/2 and WT striata. However, the DA release lasted roughly three times as long in slices from WT mice compared to slices from R6/2 mice, suggesting that R6/2 mice suffer from a depletion in the number of DA reserve pool vesicles (approximately 41.6% of WT, according to area under the curve calculations). Although the normal intracellular functions of the endogenous Htt protein are not fully understood, recent studies have shown that the expanded CAG repeat, along with promoting the formation of aggregates in neurons of both HD model mice and people who

have HD (Cooper et al., 1998; Hazeki et al., 1999; Meade et al., 2002), can also cause impairments in vesicular transport (Edwardson et al., 2003; Morton et al., 2001; Li et al., 2003). It is therefore possible that the R6/2 mice have fewer reserve pool vesicles because they are unable to transport vesicles or maintain vesicles in the reserve pool as well as WT mice.

Collectively, our data suggest that an age-dependent loss of DA reserve pool vesicles may contribute to the progressive behavioral phenotype of R6/2 mice. These findings may help guide the development of therapeutic interventions to treat chorea and other motor syndromes associated with HD. Additionally, future research efforts may be aimed at resolving the cellular mechanisms that are responsible for the depletion of the DA reserve pool.

Acknowledgments

The authors thank Prof. S. C. Fowler, University of Kansas, for advice on statistical procedures. This work was funded by the Huntington's Disease Society of America and NIH P20 RR016475 from the INBRE Program of the National Center for Research Resources.

Abbreviations

aCSF	artificial cerebral spinal fluid
AMPH	amphetamine
COC	cocaine
DA	dopamine
DAT	dopamine transporter
FSCV	fast scan cyclic voltammetry
HD	Huntington's disease
htt	huntingtin
METH	methamphetamine
αMPT	alpha-methyl-p-tyrosine
RRP	readily releasable pool
TBZ	tetrabenazine
WT	wild-type

References

- Abercrombie, ED.; Russo, ML. Program Number 195.12. in Society for Neuroscience. 2002. Orlando, FL: 2002. Neurochemistry in the R6/2 Transgenic Mouse Model of Huntington's Disease.
- Avshalumov MV, Chen BT, Marshall SP, Pena DM, Rice ME. Glutamate-dependent inhibition of dopamine release in striatum is mediated by a new diffusible messenger, H₂O₂. *J Neurosci.* 2003; 23:2744–2750. [PubMed: 12684460]
- Bates, GP.; Harper, PS.; Jones, L. Huntington's Disease. Oxford: Oxford University Press; 2002.

- Cooper JK, Schilling G, Peters MF, et al. Truncated N-terminal fragments of huntingtin with expanded glutamine repeats form nuclear and cytoplasmic aggregates in cell culture. *Hum Mol Genet.* 1998; 7:783–790. [PubMed: 9536081]
- Carter RJ, Lione LA, Humby T, Mangiarini L, Mahal A, Bates GP, Dunnett SB, Morton AJ. Characterization of progressive motor deficits in mice transgenic for the human Huntington's disease mutation. *J Neurosci.* 1999; 19:3248–3257. [PubMed: 10191337]
- Chiueh CC, Moore KE. D-amphetamine-induced release of "newly synthesized" and "stored" dopamine from the caudate nucleus in vivo. *J Pharmacol Exp Ther.* 1975; 192:642–653. [PubMed: 1120962]
- de Lange RP, de Roos AD, Borst JG. Two modes of vesicle recycling in the rat calyx of Held. *J Neurosci.* 2003; 23:10164–10173. [PubMed: 14602833]
- Edwardson JM, Wang CT, Gong B, et al. Expression of mutant huntingtin blocks exocytosis in PC12 cells by depletion of complexin II. *J Biol Chem.* 2003; 278:30849–30853. [PubMed: 12807877]
- Fischer JF, Cho AK. Chemical release of dopamine from striatal homogenates: evidence for an exchange diffusion model. *J Pharmacol Exp Ther.* 1979; 208:203–209. [PubMed: 762652]
- Floor E, Meng L. Amphetamine releases dopamine from synaptic vesicles by dual mechanisms. *Neurosci Lett.* 1996; 215:53–56. [PubMed: 8880752]
- Harata N, Ryan TA, Smith SJ, Buchanan J, Tsien RW. Visualizing recycling synaptic vesicles in hippocampal neurons by FM 1–43 photoconversion. *Proc Natl Acad Sci U S A.* 2001; 98:12748–12753. [PubMed: 11675506]
- Hazeki N, Nakamura K, Goto J, Kanazawa I. Rapid aggregate formation of the huntingtin N-terminal fragment carrying an expanded polyglutamine tract. *Biochem Biophys Res Commun.* 1999; 256:361–366. [PubMed: 10079189]
- Heien ML, Wightman RM. Phasic dopamine signaling during behavior, reward, and disease states. *CNS Neurol Disord Drug Targets.* 2006; 5:99–108. [PubMed: 16613556]
- Hickey MA, Reynolds GP, Morton AJ. The role of dopamine in motor symptoms in the R6/2 transgenic mouse model of Huntington's disease. *J Neurochem.* 2002; 81:46–59. [PubMed: 12067237]
- Hyland BI, Reynolds JN, Hay J, Perk CG, Miller R. Firing modes of midbrain dopamine cells in the freely moving rat. *Neuroscience.* 2002; 114:475–492. [PubMed: 12204216]
- Johnson MA, Rajan V, Miller CE, Wightman RM. Dopamine release is severely compromised in the R6/2 mouse model of Huntington's disease. *J Neurochem.* 2006; 97:737–746. [PubMed: 16573654]
- Johnson MA, Villanueva M, Haynes CL, Seipel AT, Buhler LA, Wightman RM. Catecholamine exocytosis is diminished in R6/2 Huntington's disease model mice. *J Neurochem.* 2007; 103:2102–2110. [PubMed: 17868298]
- Jones SR, Gainetdinov RR, Wightman RM, Caron MG. Mechanisms of amphetamine action revealed in mice lacking the dopamine transporter. *J Neurosci.* 1998; 18:1979–1986. [PubMed: 9482784]
- Kiyatkin EA, Rebec GV. Striatal neuronal activity and responsiveness to dopamine and glutamate after selective blockade of D1 and D2 dopamine receptors in freely moving rats. *J Neurosci.* 1999; 19:3594–3609. [PubMed: 10212318]
- Kulagina NV, Zigmond MJ, Michael AC. Glutamate Regulates the Spontaneous and Evoked Release of Dopamine in the Rat Striatum. *Neuroscience.* 2001; 102:121–128. [PubMed: 11226675]
- Kung MP, Canney DJ, Frederick D, Zhuang Z, Billings JJ, Kung HF. Binding of 125I-iodovinyltetrabenazine to CNS vesicular monoamine transport sites. *Synapse.* 1994; 18:225–232. [PubMed: 7855735]
- Kraft JC, Osterhaus GL, Ortiz AN, Garris PA, Johnson MA. In vivo dopamine release and uptake impairments in rats treated with 3-nitropropionic acid. *Neuroscience.* 2009; 161:940–949. [PubMed: 19362126]
- Kuromi H, Kidokoro Y. Two synaptic vesicle pools, vesicle recruitment and replenishment of pools at the *Drosophila* neuromuscular junction. *J Neurocytol.* 2003; 32:551–565. [PubMed: 15034253]
- Lape R, Dani JA. Complex response to afferent excitatory bursts by nucleus accumbens medium spiny projection neurons. *J Neurophysiol.* 2004; 92:1276–1284. [PubMed: 15331641]
- Li H, Wyman T, Yu ZX, Li SH, Li XJ. Abnormal association of mutant huntingtin with synaptic vesicles inhibits glutamate release. *Hum Mol Genet.* 2003; 12:2021–2030. [PubMed: 12913073]

- Liang NY, Rutledge CO. Evidence for carrier-mediated efflux of dopamine from corpus striatum. *Biochem Pharmacol.* 1982; 31:2479–2484. [PubMed: 7126258]
- Meade CA, Deng YP, Fusco FR, Del Mar N, Hersch S, Goldowitz D, Reiner A. Cellular localization and development of neuronal intranuclear inclusions in striatal and cortical neurons in R6/2 transgenic mice. *The Journal of comparative neurology.* 2002; 449:241–269. [PubMed: 12115678]
- Morton AJ, Faull RL, Edwardson JM. Abnormalities in the synaptic vesicle fusion machinery in Huntington's disease. *Brain Res Bull.* 2001; 56:111–117. [PubMed: 11704347]
- Neves G, Lagnado L. The kinetics of exocytosis and endocytosis in the synaptic terminal of goldfish retinal bipolar cells. *The Journal of physiology.* 1999; 515(Pt 1):181–202. [PubMed: 9925888]
- Petersén A, Puschban Z, Lotharius J, NicNiocaill B, Wiekop P, O'Connor WT, Brundin P. Evidence for dysfunction of the nigrostriatal pathway in the R6/1 line of transgenic Huntington's disease mice. *Neurobiol Dis.* 2002; 11:134–146. [PubMed: 12460553]
- Richards DA, Guatimosim C, Betz WJ. Two endocytic recycling routes selectively fill two vesicle pools in frog motor nerve terminals. *Neuron.* 2000; 27:551–559. [PubMed: 11055437]
- Richards DA, Guatimosim C, Rizzoli SO, Betz WJ. Synaptic vesicle pools at the frog neuromuscular junction. *Neuron.* 2003; 39:529–541. [PubMed: 12895425]
- Rizzoli SO, Betz WJ. Synaptic vesicle pools. *Nat Rev Neurosci.* 2005; 6:57–69. [PubMed: 15611727]
- Schwartz K, Weizman A, Rehavi M. The effect of psychostimulants on [(3)H]dopamine uptake and release in rat brain synaptic vesicles. *J Neural Transm.* 2005
- Sulzer D, Chen TK, Lau YY, Kristensen H, Rayport S, Ewing A. Amphetamine redistributes dopamine from synaptic vesicles to the cytosol and promotes reverse transport. *J Neurosci.* 1995; 15:4102–4108. [PubMed: 7751968]
- Venton BJ, Seipel AT, Phillips PE, Wetsel WC, Gitler D, Greengard P, Augustine GJ, Wightman RM. Cocaine increases dopamine release by mobilization of a synapsin-dependent reserve pool. *J Neurosci.* 2006; 26:3206–3209. [PubMed: 16554471]
- Watanabe S, Aono Y, Fusa K, Takada K, Saigusa T, Koshikawa N, Cools AR. Contribution of vesicular and cytosolic dopamine to the increased striatal dopamine efflux elicited by intrastriatal injection of dexamphetamine. *Neuroscience.* 2005; 136:251–257. [PubMed: 16181742]
- Winer, BJ. *Statistical Principles in Experimental Design.* New York: McGraw-Hill; 1962.
- Wu LG, Borst JG. The reduced release probability of releasable vesicles during recovery from short-term synaptic depression. *Neuron.* 1999; 23:821–832. [PubMed: 10482247]
- Yavich L, MacDonald E. Dopamine release from pharmacologically distinct storage pools in rat striatum following stimulation at frequency of neuronal bursting. *Brain Res.* 2000; 870:73–79. [PubMed: 10869503]
- Zucker RS, Regehr WG. Short-term synaptic plasticity. *Annu Rev Physiol.* 2002; 64:355–405. [PubMed: 11826273]

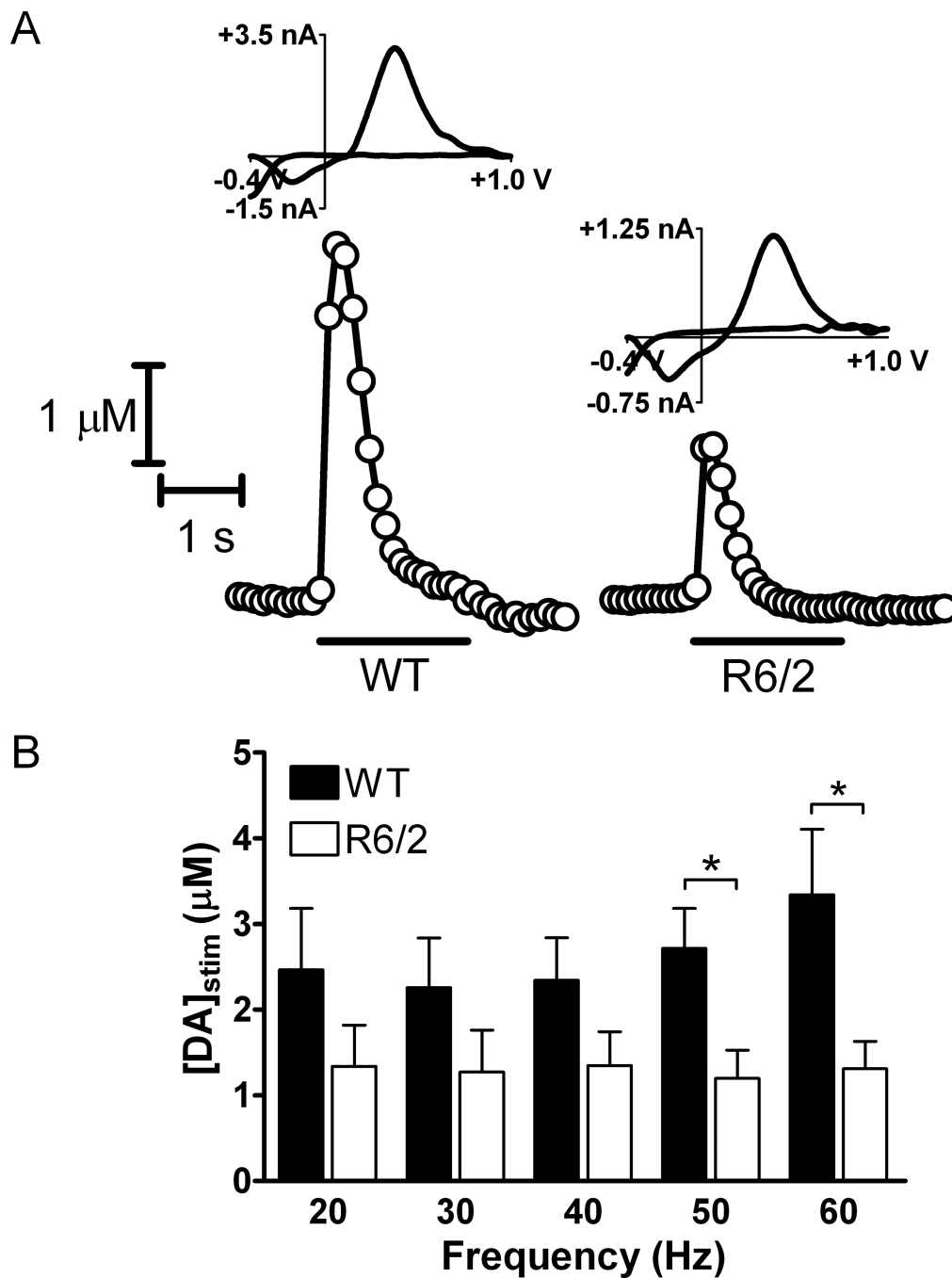


Figure 1.

Striatal DA release, evoked by the application of 120-pulse stimulus pulse trains, is impaired in R6/2 brain slices compared to WT brain slices. (A) Representative plots and cyclic voltammograms obtained by FSCV at carbon-fiber microelectrodes for R6/2 and WT mice are shown. The representative plots were taken using a 60 Hz stimulation frequency. The duration of the stimulation is represented by the bar under each plot. The cyclic voltammograms confirm the presence of DA. (B) DA release was evoked by 20, 30, 40, 50, and 60 Hz 120-pulse stimulus trains. [DA]_{stim} was significantly greater in WT brain slices compared to R6/2 brain slices when evoked using 50 Hz and 60 Hz stimulus frequencies (*p < 0.05 at 50 and 60 Hz; n = 5 R6/2

mice and 6 WT mice). Although striatal DA release appears to increase with increasing frequency in WT slices, differences in release between application frequencies are not significant within either genotype (one-way ANOVA).

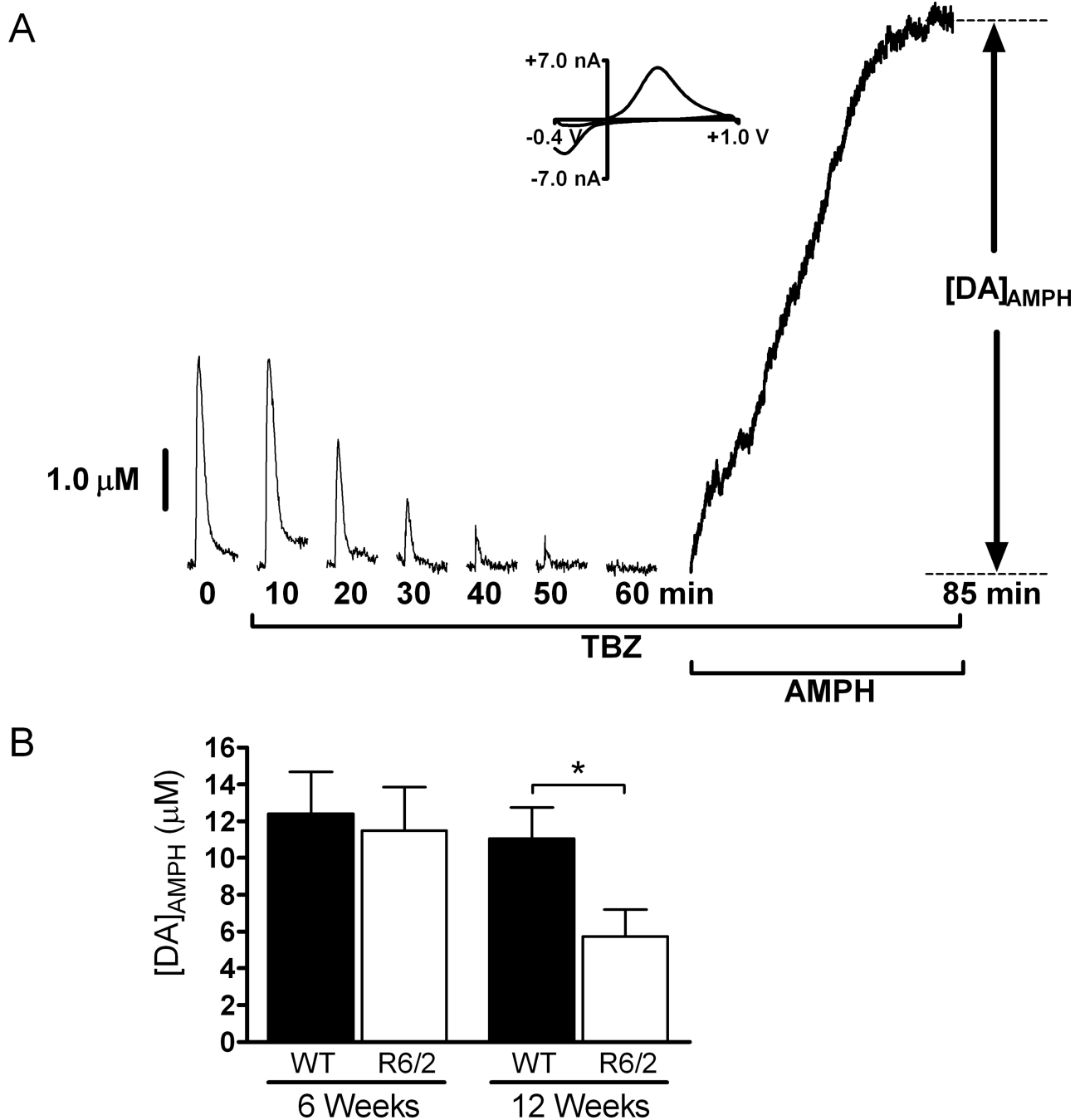


Figure 2.

AMPH induced DA efflux after TBZ treatment is impaired in 12-week old R6/2 mice compared to WT mice. (A) Representative data from a 6-week old WT mouse. The brain slice was exposed to 20 μM TBZ while applying single, 4 ms duration stimulus pulses (one pulse every 5 minutes) until DA release disappeared. The slice was then exposed to 20 μM AMPH for 25 minutes, and $[\text{DA}]_{\text{AMPH}}$ was measured. A CV is provided at peak release and confirms the presence of DA. Stimulated release plots were collected every 5 minutes, but are shown every 10 minutes for clarity. (B) In 12-week old R6/2 mice, $[\text{DA}]_{\text{AMPH}}$ is significantly less than in WT mice ($*p < 0.05$; $n = 7$ R6/2 mice and 8 WT mice), but at 6-weeks of age there is not a significant difference between the two sets of mice ($p > 0.05$; $n = 6$ R6/2 and 7 WT mice).

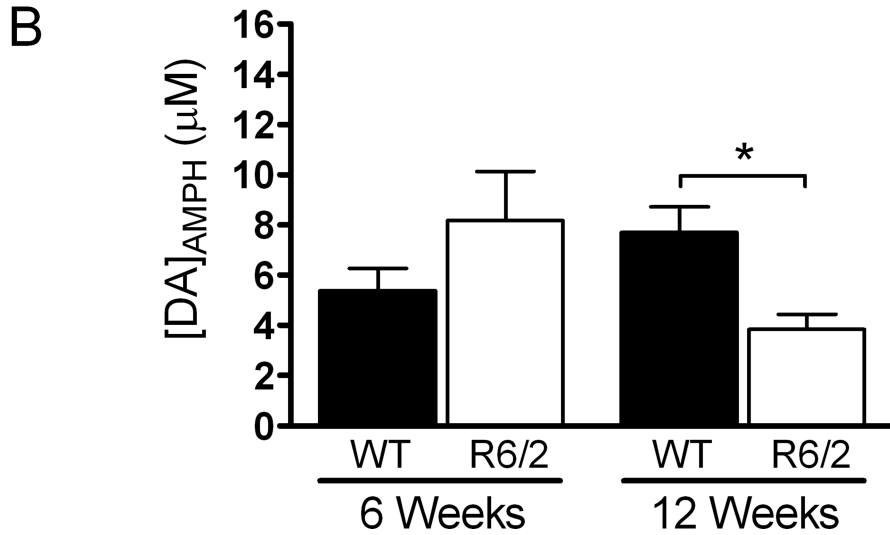
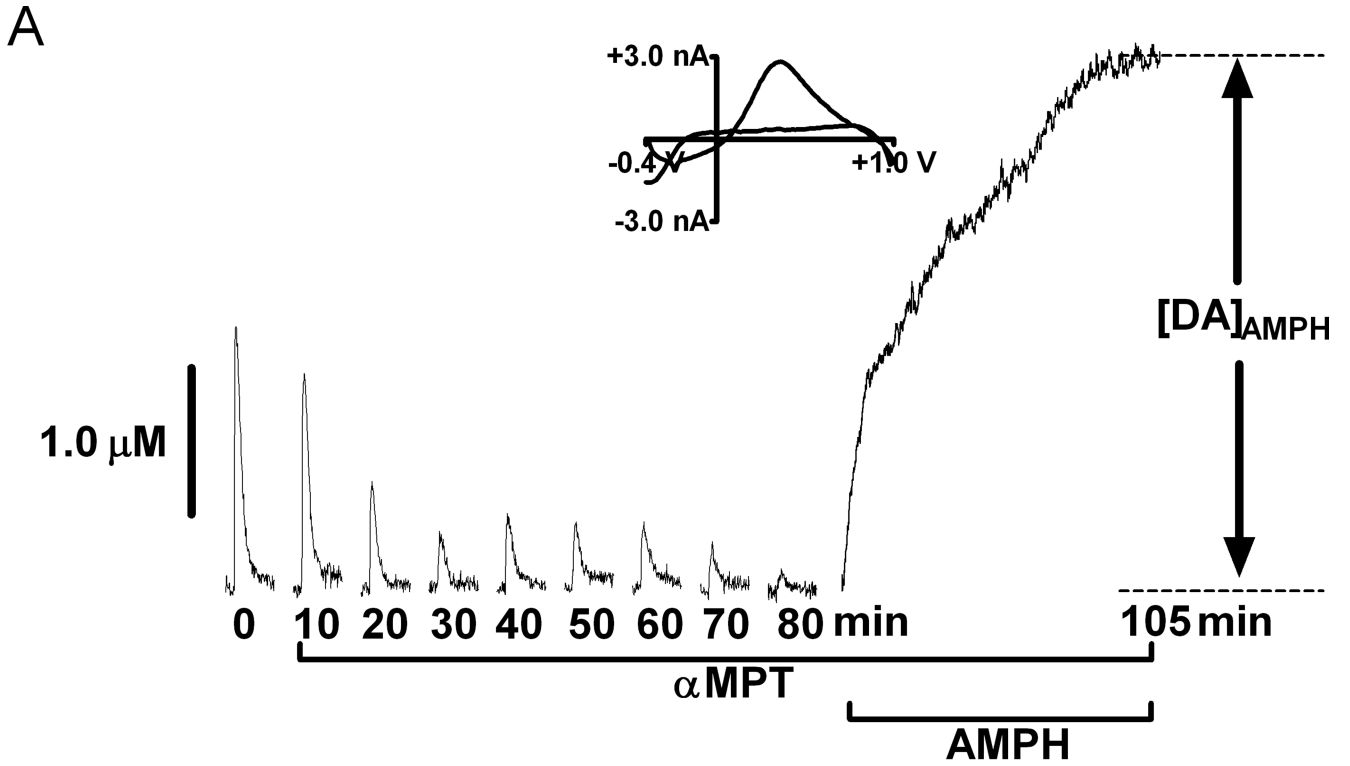


Figure 3.

AMPH induced DA efflux after α MPT treatment is diminished in older R6/2 mice. (A) Representative data from a 6-week old WT mouse. Slices were treated with 50 μ M α MPT until the stimulated DA release peak disappeared. The slice was then exposed to 20 μ M AMPH for 25 minutes and $[DA]_{AMPH}$ was measured. The last 20 minutes of AMPH treatment are shown in this particular plot. A CV is provided at peak release and confirms the presence of DA. Stimulated release plots collected every 10 minutes are shown for clarity. (B) AMPH induced DA efflux was not significantly different between 6-week old R6/2 and WT brain slices ($p > 0.05$; $n = 5$ R6/2 and 3 WT mice). $[DA]_{AMPH}$ was significantly decreased in slices from 12-week old R6/2 mice compared to those from age-matched WT control mice ($*p < 0.05$; $n = 5$ R6/2 mice and 4 WT mice).

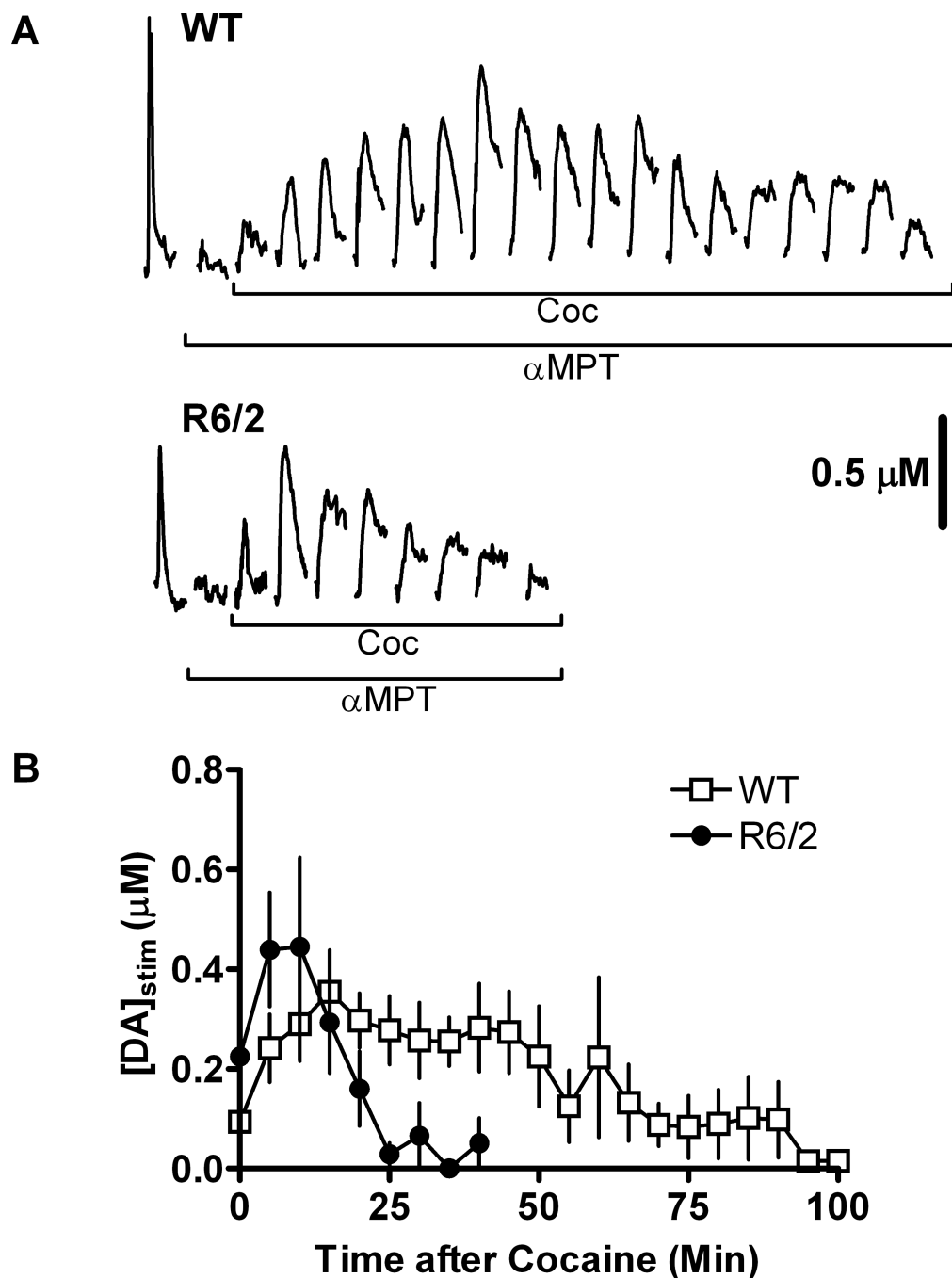


Figure 4.

Reserve pool vesicles are depleted in 12-week old R6/2 mice. Slices were treated with 50 μ M α MPT while applying a 4 ms duration single-pulse electrical stimulus every 5 minutes. Once the stimulated DA release peak disappeared, 20 μ M COC was added to the brain slice and the application of stimulus pulses continued. Stimulated DA release was measured by FSCV. (A) Representative data from R6/2 and WT slices. Reserve pool mobilization by COC resulted in measurable stimulated DA release. Stimulated release plots collected immediately after the addition of α MPT and the disappearance of the DA release peak have been omitted in this figure for clarity. (B) Pooled data from R6/2 and WT mice. Each data point represents the average value (\pm

SEM) of $[DA]_{stim}$ obtained from 5 R6/2 mice and 6 WT mice. The maximum peak amplitudes obtained in R6/2 and WT slices were not significantly different.